IN VITRO EVALUATION OF ANEURYSMAL HEMODYNAMICS AFTER ITS ENDOVASCULAR BYPASS BY FLOW DIVERTORS

B.B. Lieber*, **, J. Seong* and A.K. Wakhloo***

* University of Miami/Department of Biomedical Engineering, Coral Gables, USA
** University of Miami/Department of Radiology, Miami, USA
*** University of Massachusetts Medical School/Department of Radiology, Worcester, USA

blieber@miami.edu

Abstract: The objective of endovascular treatment of cerebral aneurysm is to exclude them from the circulation. Flow divertors, which are stent-like devices, can serve as adjunct to coils or stand alone bioimplants for treatment of cerebral aneurysms. Currently there are only a few stents available that can negotiate the tortuous cerebrovasculature. However, these have been designed only as scaffolds for coils. To successfully exclude an aneurysm from the circulation by a flow divertor alone, the design parameters, such as porosity and pore density (or filament diameter), have to be tailored to the local hemodynamics for long term success of treatment. This study investigates the influence of a flow divertor on intra-aneurysmal flow. The divertor was placed in the parent artery traversing the neck of the aneurysm. The aneurysm was molded of a silicone elastomer with a geometry representative of the elastase-induced saccular aneurysm model in rabbit. The results show that flow divertors significantly reduce flow activity inside the aneurysm. After flow divertors were implanted in the model, the mean hydrodynamic circulation inside the aneurysm was reduced to about 13% of its pre-divertor value. Therefore, flow divertors can induce sufficient flow stasis inside the aneurysm and possibly trigger spontaneous thrombosis.

Introduction

Flow divertors can be used as an alternative to coils in endovascular treatment of human brain aneurysms for their exclusion from the cerebral circulation. Flow divertors can redirect flow into the parent vessel distally, away from the aneurysm, thereby reestablishing physiological flow patterns. The decoupling of the aneurysm from the parent vessel flow impedes flow activity inside the aneurysm to such a degree that it may spontaneously thrombose. For exclusion of an aneurysm from the circulation by a flow divertor its design parameters, such as porosity and filament diameter, have to be tailored to the local hemodynamics for long term success of the bioimplant.

The hemodynamic efficacy of flow divertors in this study was tested in an elastomeric *in vitro* model of elastase-induced saccular aneurysm in the rabbit right common carotid artery (CCA). The elastase-induced aneurysm model in rabbit was developed as an *in vivo* model of a human cerebral aneurysm, and it can be used for testing various endovascular devices and therapies. The aneurysm is constructed endovascularly in the root of the right CCA, which approximates the size of the human middle cerebral artery. Therefore, the created aneurysm is similar to those found in humans around the main branches of the circle of Willis.

Materials and Methods

Experimental *in vivo* aneurysms were created in New Zealand white rabbits weighing 3-4 Kg [1]. A pre anesthetic agent, glycopyrrolate (0.01 mg/kg of body weight), was first injected intramuscularly followed by injection of ketamine (35 mg/kg) and xylazine (5 mg/kg) to induce anesthesia that was maintained thereafter by inhalation of 1.0-1.5 % isoflurane. A heating pad was used to maintain the animal body temperature at 37.5°C during the procedure. After induction of anesthesia, the hair over the neck was shaved and the right CCA was isolated. A 5 Fr introducer sheath was placed in the right CCA retrogradely. A balloon catheter was advanced through the sheath, positioned at the origin of the right CCA, and inflated. A microcatheter was advanced side-by-side with the shaft of the balloon catheter. A solution containing 50 units of porcine pancreatic elastase mixed with contrast (for visualization) was incubated in the dead space segment of the right CCA, above the inflated balloon, for approximately 20 minutes. Following the incubation period, the elastase was aspired and the right CCA was ligated above the access port. Aneurysms were allowed to mature for 21 days and following maturation of the aneurysm each animal underwent follow-up angiography to document the model. Figure 1 shows the aneurysm model and its surrounding vasculature before and after induction together with a resin cast of the aneurysm that was obtained at sacrifice.

Measurements of the geometry of the elastase-induced aneurysms in rabbit were used to obtain an average representative geometry [1]. The representative geometry was used to construct a compliant silicone model of the aneurysm and the surrounding vasculature for *in vitro* testing. The *in vitro* models were fabricated by advanced rapid prototyping techniques. Older molding techniques for fabricating high fidelity

ISSN: 1727-1983

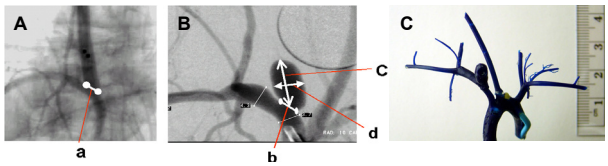

Figure 1: A: Angiogram showing the diameter of the origin of the common carotid artery (a) measured immediately after elastase incubation. B: Aneurysm three weeks after induction; b - neck width, c - dome height, d - dome width. C: A resin cast of an elastase-induced aneurysm in rabbit

compliant replicas of arterial beds, specific to an individual, often involve the use of fresh human cadavers and require highly developed casting skills [2]. Recently, we employed rapid prototyping techniques for creating compliant arterial models using arterial luminal data from CT and MRA [3]. However, due to the high variability in the geometry of elastase-induced aneurysms in rabbits, in this study we opted to use an average representative geometry of the animal model. The average geometry was generated by multiple measurements on experimental aneurysms *in vivo*. Nonetheless, case-specific compliant replicas of arterial beds, rather than the use of a geometrical average, can be fabricated from three dimensional images of vascular lumens obtained using our rotational angiography system (Siemens Angiostar, Forchheim, Germany).

The geometrical-average model of the elastase-induced aneurysm in rabbit was designed in Pro/Engineer 2001 (PTC, Needham, MA), and fabricated using a rapid prototyping system (Prodigy Plus, Stratasys Inc., Eden Prairie, MN). This system uses Fused Deposition Modeling (FDM) whereby Acrylonitrile Butadiene Styrene (ABS) cast material and a support material (WaterWorks) are molten in a computer controlled extrusion head and deposited in layers of 178 µm thickness. The WaterWorks support structure is removed from the fabricated mold using a jet-action cleaning bath (CleanStation, PM Technologies, Minneapolis, MN). WaterWorks melts out completely in a sodium hydroxide aqueous solution (Sodium Hydroxide - P400SC, Stratasys Inc.) at a temperature of 150°F.

The ABS core that remains after removal of the support structure serves as a mold that is coated with an elastomer. However, to obtain optical clarity of the final

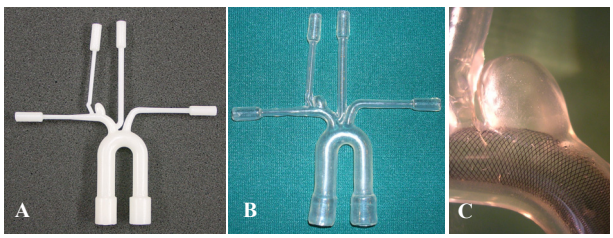

Figure 2: A: ABS mold of the elastase-induced aneurysm model. B: Elastomeric model fabricated from coating the ABS mold shown in A. C: A model with a flow divertor implanted

elastomeric product the surface of the ABS mold has to be smoothed before coating. To obtain a surface as smooth as possible, the mold was dipped in solvent (Xylene XY-24, KleanStrip, Memphis, TN) for a short period of time, removed, and allowed to dry at room temperature. During the drying period while solvent was evaporating, the surface was smoothed due to shallow melting. Final polishing of the surface was achieved using fine grit sandpaper and a Dremel tool set (Model No 395 - Robert Bosch Tool Corporation, Mount Prospect, IL).

A silicone elastomer (Silbione 40000, Rhodia Silicones, Ventura, CA) was used to dip-coat the mold. The desired thickness of the final product was achieved by applying four coats at hourly intervals. Uniform coating of the elastomer was achieved by mounting the coated mold on an AC/DC gear motor (Model No. 2Z802B - Dayton, St. Louis, MO) and spinning it about both the horizontal and vertical axes. The rotation speed was varied between 4 and 130 rpm. For final curing the elastomer was placed in a vacuum oven (Model No 1430 - VWR, West Chester, PA) at 50°C for 8 hours, followed by another 8 hours at 70°C. After the curing process was complete the ABS core was dissolved by immersing it in a bath of solvent for a period of 24 hours. Following complete dissolution of the ABS core the compliant silicone replica was removed from the solvent bath and air-dried at room temperature for 24 hours. Figure 2B shows an example of a vascular replica fabricated using the procedure described above.

To mimic the aortic flow waveform of the rabbit in the experimental flow apparatus, the ascending aortic flow waveform was measured in an anesthetized New Zealand White rabbit weighing 4 kg. The following experimental protocol was implemented to obtain the flow waveform in the ascending aorta of the rabbit. Preparation of the animal and induction of anesthesia was performed as described above. After induction of anesthesia the hair over the chest was shaved and the animal was kept on heating pad (37.5 ºC). The animal was mechanically ventilated (Harvard Apparatus Co. Inc., Mills, MA) at 40 strokes per minute with a tidal volume of 25 to 30 ml of oxygen. A perivascular flow probe (5R B23, Transonic System Inc., Ithaca, NY) was placed around the ascending aorta. Heart rate and blood pressure were allowed to stabilize and maintained constant throughout the procedure. Measurements of the aortic flow were taken with a transit time ultrasonic flowmeter (T206, Transonic Systems Inc, Ithaca, NY) connected to the perivascular probe. The output of the flowmeter was recorded on a data acquisition computer equipped with a data acquisition board and associated software (Virtual Bench V. 2.0, National Instruments Co., Austin, TX).

For the *in vitro* study, the measured flow waveform in the rabbit was amplified and fed into a computer controlled reciprocating piston pump (CompuFlow 1000, Shelly Medical Imaging Technology, Ontario, Canada). Waveform amplification was required in order to match the hemodynamic similarity parameters, namely, the Reynolds and Womersley numbers, in the scaled-up elastomer model (scaling factor 1.36) to those

ISSN: 1727-1983

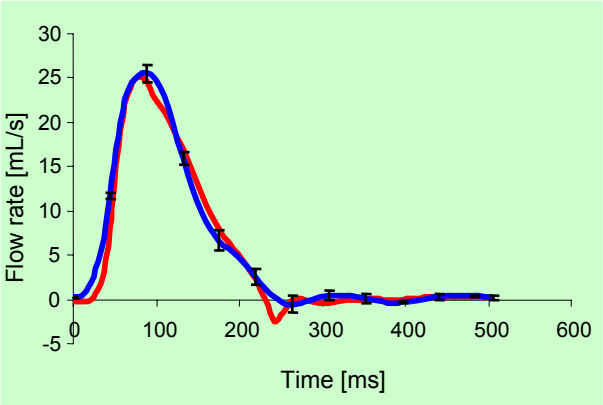

Figure 3: Modified flow rate in the ascending aorta of the anesthetized rabbit (—). Flow rate (—) in the ascending aorta of the elastomer model (error bars denote SEM)

found in the rabbit. The amplification of the waveform programmed into the pump was adjusted to achieve a peak systole Reynolds number of 971 and a Womersley number of 9.4 at the ascending aorta of the *in vitro* compliant model. The amplified flow waveform in the ascending aorta of the rabbit (amplification factor 1.38) that served as input waveform to the pump is shown Figure 3 together with the resulting flow waveform in the ascending aorta of the elastomeric model.

A water-glycerol mixture (41:59 by volume) was used to obtain refractive index matching (1.411) between the working fluid and the elastomer model at a working temperature of 50ºC. The compliance of the model yielded a 10% change in the caliber of the ascending aorta of the silicone model when subjected to systolic/diastolic pressure changes. The flow was analyzed using a particle image velocimetry (PIV) system [4]. Two divertors of different porosity but of the same filament diameter (Table 1) were investigated. Each divertor was carefully inserted into the silicone model (Figure 2C) and intra-aneurysmal flow investigated before and after its implantation. The divertor was then removed from the model and the process was repeated for the other divertor.

Table 1: Specifications of flow divertors

	Filament Diameter	Porosity
Divertor A	38 µm	71%
Divertor B	38 µm	65%

Results

Pre-divertor (left column of Figure 4, (1a-1e)), flow in the bottom area of the aneurysm rotates counter-clockwise during early systole. During late systole the vortex inside the aneurysm changes to clockwise rotation and intensifies. The clockwise rotation inside the aneurysm continues well into the diastolic period during the flow cessation phase in the parent vessel. Post-divertor (right column of Figure 4 (2a-2e)), a significant reduction in the magnitude of the flow inside the aneurysm during both systole and diastole can be

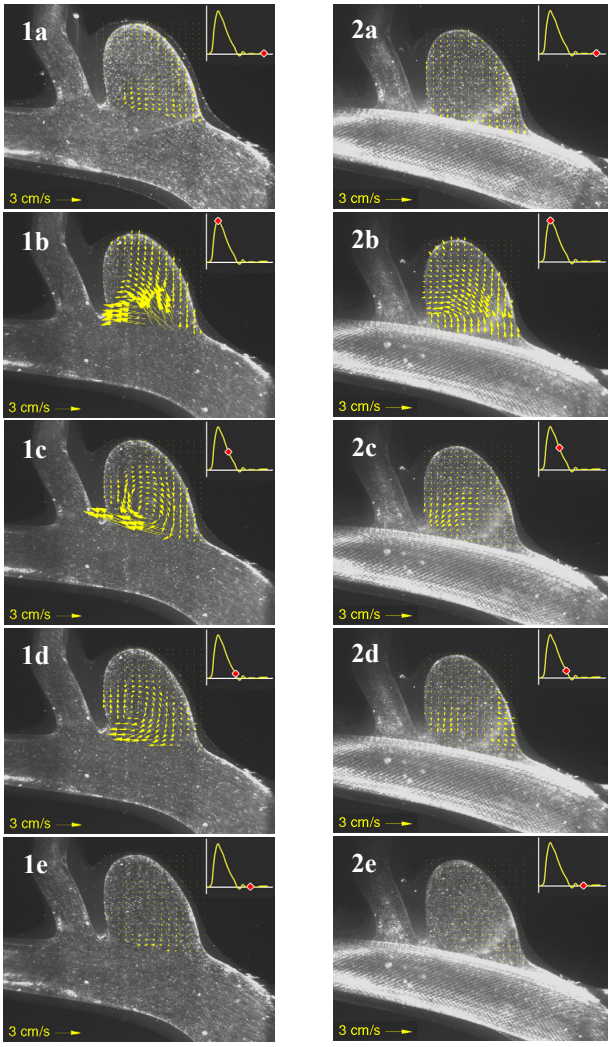

Figure 4: PIV flow patterns in the elastomeric aneurysm model of the elastase-induced aneurysm model in rabbit. Panels 1a-1e before implantation of a flow divertor, and panels 2a-2e after implantation of flow divertor A

observed. From end diastole to early systole there is virtually no flow in the aneurysm (panels 2a and 2e). From early systole to peak systole flow is confined to only the bottom portion of the aneurysm (panel 2b). During late systole to early diastole (panels 2c and 2d) flow in the aneurysm continues in counter-clockwise

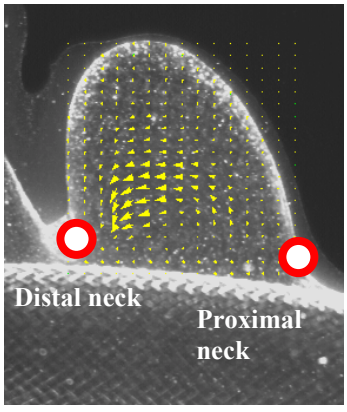

Figure 5: Proximal and distal neck of the aneurysm where local wall shear rate was measured

ISSN: 1727-1983

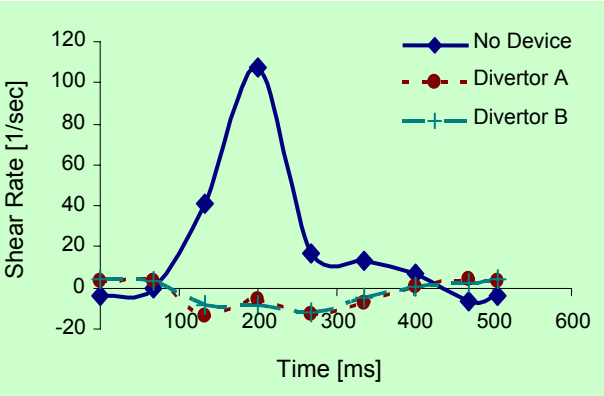

Figure 6: Shear rate at the distal neck of the aneurysm before and after flow divertor implantation

direction in contradistinction to its direction of rotation during the same period in the pre-divertor (or control) case except in the vicinity of the proximal neck where flow exits in a clockwise fashion due to the recoil of the aneurysm wall during diastole. Nonetheless, vortex velocities are much smaller than in the control.

Pre-divertor, during peak systole intra-aneurysmal flow is counterclockwise and fast in the vicinity of aneurysm neck. However, post-divertor flow in the same area is slow and diffused. This reduction and redistribution of the flow reduces the wall shear rate at the distal and proximal neck of the aneurysm (Figure 5). Large oscillations in direction and magnitude of the wall shear stress at the neck of the aneurysm are believed to play a major role in aneurysm growth and possibly in subsequent rupture. Figure 6 shows the temporal evolution of shear rate adjacent to the distal neck of the aneurysm. Both flow divertors significantly reduce the shear rate and reverse its direction. At the proximal neck (Figure 7) shear rate magnitude is also reduced, however, direction of the shear post-divertor remains in phase with its direction in the control.

Instantaneous intra-aneurysmal vorticity was evaluated throughout the cardiac cycle and the instantaneous hydrodynamic circulation was calculated from the vorticity. The temporal evolution of the circulation inside the aneurysm pre- and post- both divertors is shown in Figure 8. Markedly different behavior for the hydrodynamic circulation pre and post

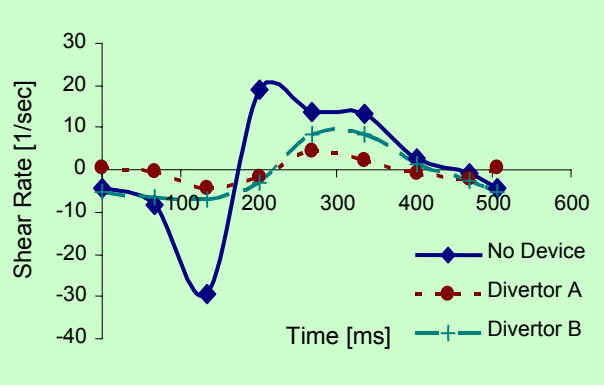

Figure 7: Shear rate at the proximal neck of the aneurysm before and after flow divertor implantation

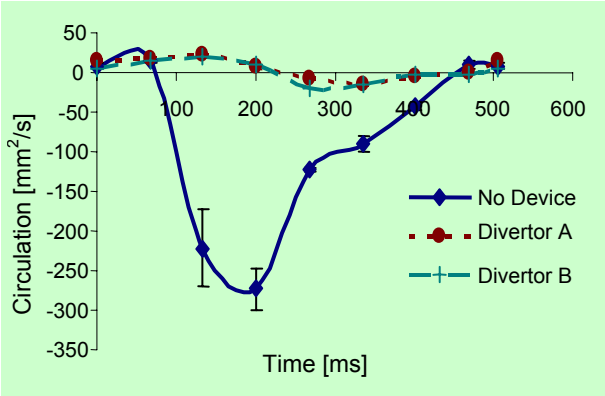

Figure 8: Temporal evolutions of intra-aneurysmal circulation (error bars denote SEM)

divertor can be observed. Post-divertor the hydrodynamic circulation is greatly diminished. The time average of the hydrodynamic circulation was determined from its distribution throughout the pulsatile cycle (Figure 9). The results demonstrate that post-divertor the mean hydrodynamic circulation was reduced to less that 13% of its value in the control. These results show that flow divertors can induce sufficient flow stasis inside the aneurysm and possibly trigger spontaneous thrombosis.

One of the notable differences between the cerebral and the systemic circulation is the bypass of hierarchical branching in supplying brain tissue. Small blood vessels that penetrate brain tissue emanate from large feeding arteries that are a few generations larger. These blood vessels are commonly named perforators and maintaining blood flow through them is vital to the brain. When placing a flow divertor over the neck of an aneurysm, entrance to adjacent perforators may be crossed by the divertor, a phenomenon commonly referred to as jailing. Some concern has been raised in the past whether jailing of perforators may lead to their

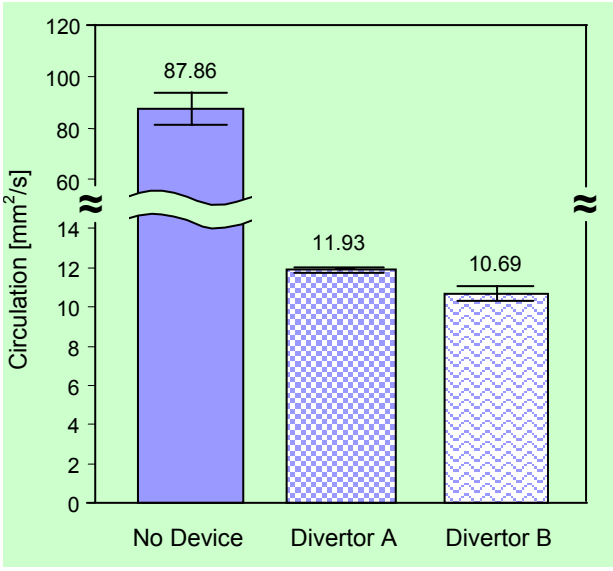

Figure 9: Mean hydrodynamic circulation in the aneurysm before and after flow divertor implantations (error bars denote SEM)

ISSN: 1727-1983

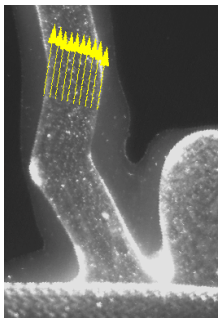

Figure 10: Velocity vectors in the vertebral artery of the silicone model

occlusion. Therefore, we have examined the flow rate in the vertebral artery of the elastomer model, which represents a perforator. The pulsatile flow velocity in the perforator was measured before and after its origin was crossed by the mesh of the flow divertor (Figure 10). The instantaneous flow rate through the perforator was obtained by integrating the velocity profile, and the average flow rate was obtained by integrating the pulsatile flow waveform. The results show that mean flow rate through the vertebral artery for each of the two implanted divertors was reduced by 8% of the corresponding flow rate before divertor implantation (Figure 11). This reduction shows that there is a slight increase in the hydraulic resistance to flow into the perforator, but this increase does not adversely affect the flow through the perforator.

Conclusions

Implantation of flow divertors in the parent artery that traverse the aneurysm neck can significantly reduce flow activity inside the aneurysm sac. The shear rate in the vicinity of the aneurysm neck is reduced, particularly at the distal neck that acts as a flow divider to the oncoming flow. While the mechanisms of aneurysm growth and rupture are unclear, high oscillatory shear at the neck of the aneurysm, which changes its direction in the course of the heart beat, has been proposed as one of the possible mechanisms responsible for aneurysm growth [5]. Reduction in the magnitude of the wall shear oscillations can, in itself, help in preventing further aneurysm growth and lower its eventual rupture potential.

The mean circulation after divertor implantation was reduced to only 13 % of mean circulation before implantation in both cases. In contradistinction, the mean flow rate in the perforator after divertor placement in the parent artery across its origin did not change appreciably post-implantation as compare to the control. The time averaged flow rate in the vertebral artery after jailing remained more than 90% of its pre-divertor flow rate. These results are not unexpected since flow through a perforator jailed by a porous medium is driven by the pressure gradient between the entrance and the terminus (or the vein). In contradistinction, an aneurysm lacks a low pressure exit port and flow has to emanate from the same opening it entered. Therefore,

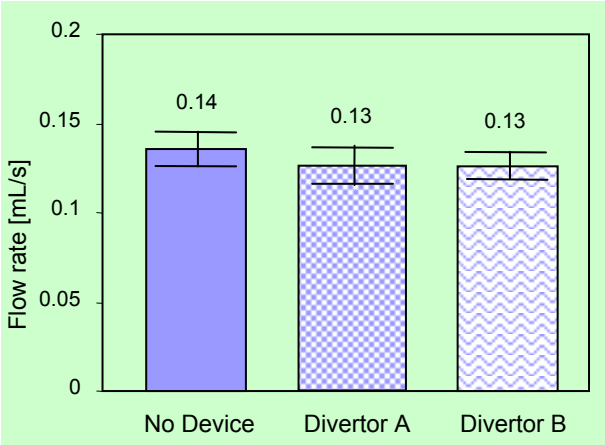

Figure 11: Mean flow rate in the vertebral artery before and after implantation of flow divertors (error bars denote SEM)

flow cessation in the aneurysm sac due to placement of a porous divertor across its neck is more likely to occur.

Acknowledgements

This work was supported by the National Institutes of Health under grant R01 NS045753-01A1.

References

[1] ONIZUKA M., MISKOLCZI L., GOUNIS, M. J., SEONG J., LIEBER B. B., and WAKHLOO A. K. (2005): 'Elastase-Induced Aneurysms in Rabbits - Effect of Post-Construction Geometry on Final Size', *AJNR Am. J. Neuroradiol.* (in press)

[2] KERBER C. W., HEILMAN C. B., and ZANETTI P. H. (1989): 'Transparent elastic arterial models. I: A brief technical note'. *Biorheology,* **26(6),** pp.1041-49

[3] SEONG J., LIEBER B. B., WAKHLOO A. K. (2004): 'Compliant silicone elastomer models of elastase-induced aneurysms in the rabbit: model construction and hemodynamics', Proc. of 2004 ASME IMECE, Anaheim, CA, USA, 2004, Abst. No. 59467

[4] LIEBER B. B., LIVESCU V., HOPKINS L. N., and WAKHLOO A.K. (2002): 'Particle image velocimetry assessment of stent design influence on intra-aneurysmal flow', *Ann. Biomed. Eng.,* **30**, pp. 768-777

[5] WAKHLOO, A. K., LIEBER, B. B., SANDHU, J. S., GOUNIS, M. J. (2004): 'Flow Dynamics in Aneurysms', in: LEROUX, P.D., WINN, H.R., NEWELL, D.W. (Eds): 'Management of Cerebral Aneurysms', (W.B. Saunders, Philadelphia), pp. 99-120

ISSN: 1727-1983